

①

COMPONENT PART NOTICE

THIS PAPER IS A COMPONENT PART OF THE FOLLOWING COMPILATION REPORT:

TITLE: Proceedings of the U.S. Army Symposium on Gun Dynamics (7th)

Held in Newport, Rhode Island on 11-13 May 1993.

TO ORDER THE COMPLETE COMPILATION REPORT, USE AD-A278 075.

THE COMPONENT PART IS PROVIDED HERE TO ALLOW USERS ACCESS TO INDIVIDUALLY AUTHORED SECTIONS OF PROCEEDING, ANNALS, SYMPOSIA, ETC. HOWEVER, THE COMPONENT SHOULD BE CONSIDERED WITHIN THE CONTEXT OF THE OVERALL COMPILATION REPORT AND NOT AS A STAND-ALONE TECHNICAL REPORT.

THE FOLLOWING COMPONENT PART NUMBERS COMPRISE THE COMPILATION REPORT:

AD#: AD-P009 060 AD#: _____

AD#: thru AD#: _____

AD#: AD-P009 091 AD#: _____

Accession For	
NTIS CRA&I	<input checked="" type="checkbox"/>
DTIC TAB	<input checked="" type="checkbox"/>
Unannounced	<input type="checkbox"/>
Justification _____	
By _____	
Distribution /	
Availability Codes	
Dist	Avail and/or Special
<u>A-1</u>	

DTIC
ELECTE
MAY 17 1994
S G D

BURTON

**TITLE: AN EXAMINATION OF IN-BORE PROJECTILE
MOTION FROM AN EM RAILGUN**

AD-P009 068



**LARRY BURTON
U.S. ARMY RESEARCH LABORATORY
WEAPONS TECHNOLOGY DIRECTORATE
ABERDEEN PROVING GROUND, MD 21005-5066**

ABSTRACT:

An investigation was undertaken to examine electromagnetic (EM) gun barrel/projectile interaction. The RASCAL code was used in this study because of its ability to easily manipulate relevant parameters such as gun tube centerline, projectile/bore contact stiffness, and projectile design geometry. This work centers around a comparison of projectile performance in the 9-MJ EM railgun at the University of Texas Center for Electromechanics (UTCEM) and a double-travel conventional gun. This comparison was made by varying the parameters listed above for two different projectile designs, one projectile being the M829 tank round, the other, a preliminary EM design. It was hoped that adoption of this format would identify specific areas of the EM gun/projectile system that excite transverse loading, with the results of the analysis presented here.

BIOGRAPHY:

PRESENT ASSIGNMENT: Mechanical Engineer, Mechanics & Structures Branch, Propulsion & Flight Division, Weapons Technology Directorate, U.S. Army Research Laboratory.

PAST EXPERIENCE: Nine years with the Mechanics & Structures Branch.

DEGREES HELD: M.S. (Mechanical Engineering), The Johns Hopkins University, Baltimore, MD, 1992; B.S. (Mechanical Engineering), Virginia Polytechnic Institute and State University, Blacksburg, VA, 1984.

94-14463



BENEDETTI

Therefore, to prevent the spinning projectile from turning upside down during parachute descent, the projectile center of gravity (CG) must be located aft of the center of pressure (CP_{mag}) for the Magnus force. This, of course, applies to the post parachute deployment projectile configuration.

REFERENCE

1. Benedetti, G. A., *Flight Dynamics of a Spinning Projectile Descending on a Parachute*, Sandia National Laboratories Livermore, SAND89-8419, 1989.

An Examination of In-bore Projectile Motion from an EM Railgun

Larry Burton
U.S. Army Research Laboratory
Weapons Technology Directorate
Aberdeen Proving Ground, MD 21005-5066

INTRODUCTION

During the past decade, it has been recognized that a projectile's interaction with the gun tube during in-bore travel plays a major role in determining the terminal accuracy of the round. If the projectile is subjected to excessive transverse loading during this period, disturbances may be induced that lead to yawing motion and possibly even excitation of the projectile's natural frequencies. Obviously, it is important for the projectile designer to minimize the effects of these occurrences.

In recent years, much effort has been devoted to developing modeling techniques that may be used to estimate the disturbances that arise from projectile/gun tube interaction. These models range in scope from a one-dimensional beam element code, RASCAL [1], to three-dimensional, transient analysis with commercial finite element programs. The use of these techniques to investigate gun/projectile dynamics in conventional tank cannons is well documented [2,3,4,5,6].

Currently, however, there are ongoing programs to develop alternatives to conventional powder guns. One example is the electromagnetic (EM) gun system, which relies on passing current through an armature in an induced magnetic field to provide its propulsive force. The EM gun barrels are composite in nature, that is, having a non-homogeneous cross section (see Figure 1). This is a radical departure from the cylindrical steel tubes characteristic of current cannons. In addition, solid armature railguns typically rely on metal-to-metal contact to conduct current between the gun rails and the armature, which leads one to believe the EM system has characteristics that may lead to more excessive transverse disturbances being imparted to the projectile.

An analysis was undertaken to determine the severity of transverse loading in an EM barrel in comparison to a conventional steel gun tube. The details of the analytical investigation and the subsequent results are presented in the following sections.

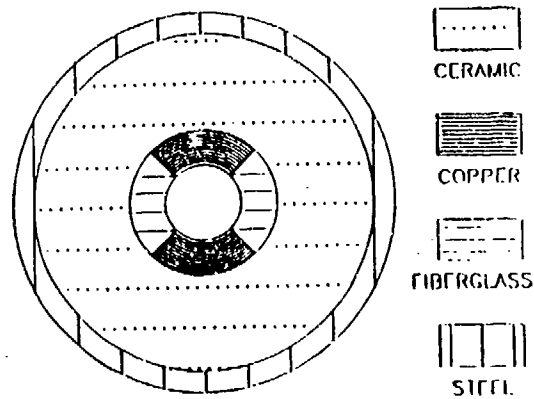


Figure 1. EM Railgun Barrel Cross Section

PURPOSE

The purpose of the analytical investigation was to determine the severity of transverse loading in an EM barrel in comparison to a conventional steel gun tube. It was hoped that by running numerous case studies while varying the parameters affecting in-bore projectile motion, a cause-and-effect relationship could be identified and the most deleterious conditions isolated.

PROCEDURE

Realizing the gross difference between conventional and EM gun systems, it was felt advantageous to exercise a simplistic in-bore dynamics code, which would allow for easy manipulation of the relevant parameters. This led to the RASCAL code [1] being chosen as the vehicle for conducting the investigation. RASCAL is a one-dimensional code, which employs beam elements and requires inputs of interior ballistic loading information, projectile geometry, barrel dimensions and centerline profile, and breech and gun system parameters. The specific values incorporated into the model are detailed in the following sections.

GUN BARREL MODELING

The study focused on a comparison of projectile motion in an EM railgun with that of a conventional gun. The 9-MJ railgun at the University of Texas Center for Electromechanics (UTCEM) was selected as the railgun gun to be modeled because centerline data for the barrel exists. The existence of centerline data is noteworthy for the EM community has only recently begun to recognize the important role the centerline profile plays in determining in-bore motion. It is also important to note the centerline profile changes drastically from shot to shot with current state-of-the-art railguns. Railguns are typically honed out after every shot to remove damage done by arcing and wear, thus placing the in-bore geometry in a continual state of fluctuation. Thus, the data employed in the model are a one-time barrel centerline meant to be representative of that found in the UTCEM gun.

The UTCCEM gun is 9.5 m long and is mounted vertically. It has a constant diameter cylindrical cross section along its entire length. A double-travel conventional gun was chosen to serve as a comparator because its 10-m length is nearly equivalent to that of the UTCCEM barrel and allows for velocities above those of standard ordnance. The gun barrel geometries are depicted below in Figure 2.

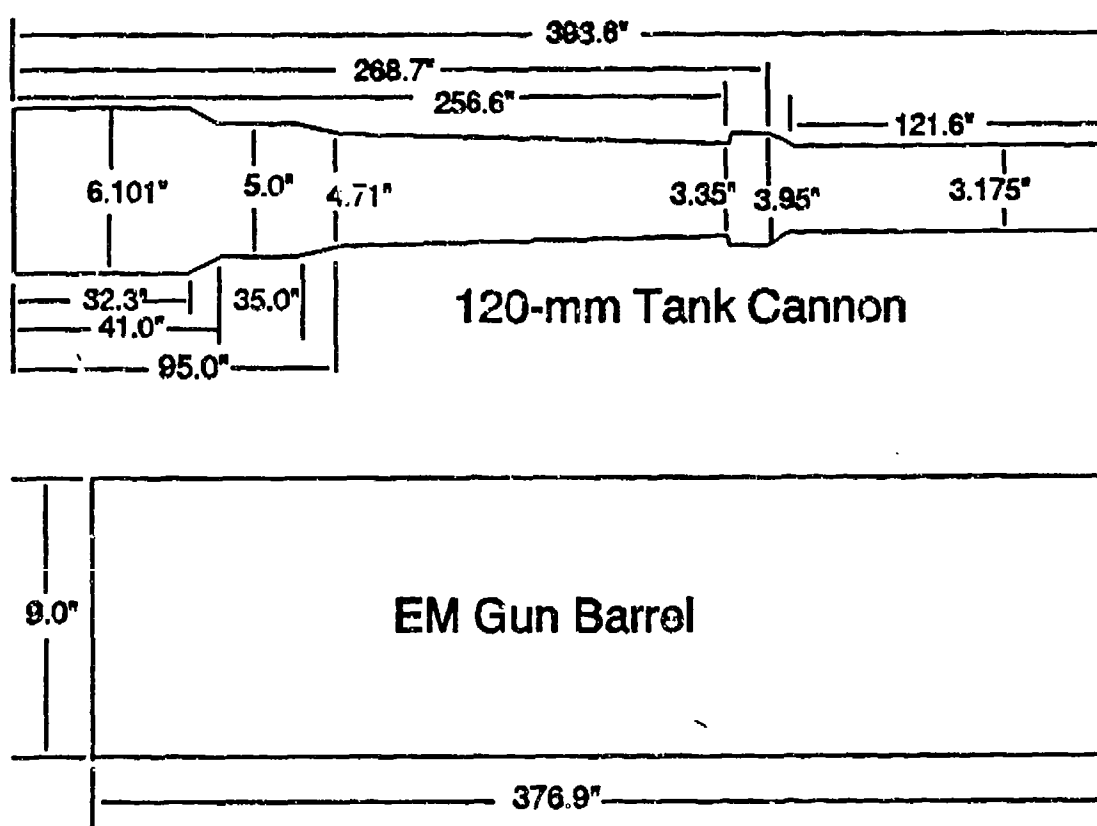


Figure 2. Barrel Geometries of EM and Double-Travel Guns

Note: the two barrels modeled have different bore diameters; the EM railgun has a 90-mm nominal diameter, while the double-travel cannon is 120 mm. One of the benefits of RASCAL is it does not require barrel geometry to be consistent with projectile geometry. In other words, it is possible to examine the motion of a 120-mm projectile in a 90-mm bore and vice versa. This capability results from RASCAL's use of beam elements to model the projectile with the projectile/barrel contact points represented with springs.

Figure 3 shows the centerline data incorporated into the gun barrel models. For the EM railgun, the vertical measurements are for the plane of the copper rails, while the horizontal are for the ceramic insulator. Tube 008 data refer to the double-travel cannon, and data line 2 simply is a verification of the original measurements of the UTCCEM gun shown as data line 1.

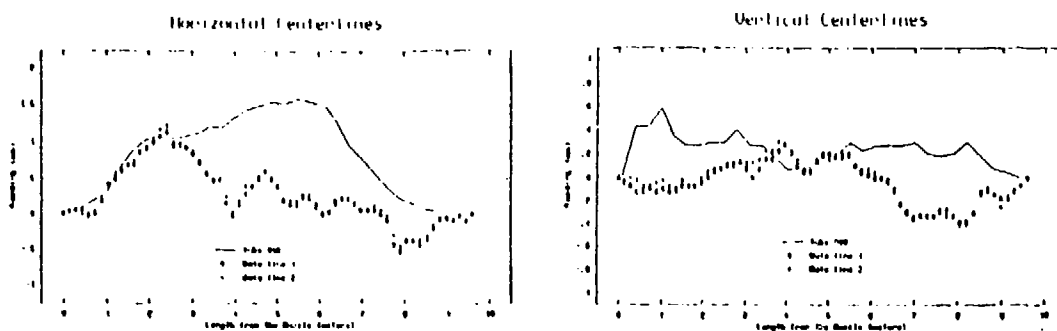


Figure 3. Gun Barrel Centerline Measurements

The final input requirement pertaining to the barrels was descriptions of the breech and gun system parameters. Since both guns are experimental, that is, not meant to be mounted in any vehicle, it was decided to use identical input files for the two guns except for bore and chamber radii particular to each gun, as well as the elastic modulus and material density of the barrels.

Obviously, for the case of the homogeneous steel conventional gun, the modulus ($30 \times 10^6 \text{ lb/in}^2$) and density (0.283 lb/in^3) are known. The EM barrel is not as straightforward for the laminate nature of its cross section calls for derivation of an effective modulus and density. An effective density was calculated using a simple rule of mixtures approach, whereby the density of each material layer was multiplied by its volume and these values were summed to give the total weight of the barrel. This weight was then divided by the total volume of the barrel to provide an effective density of the barrel (0.193 lb/in^3). A similar method was used to derive an effective modulus using a beam-deflection analysis. If each layer is considered a beam that maintains contact with its adjacent layer, the deflections are equivalent at coincidental points and have values of the form $y = (wl^4)/(8EI)$. This leads to

$$Y_1 = Y_2 = Y_3 = \frac{w_1 l^4}{8E_1 I_1} = \frac{w_2 l^4}{8E_2 I_2} = \frac{w_3 l^4}{8E_3 I_3} = Y_{\text{eff}} = \frac{w_{\text{eff}} l^4}{8E_{\text{eff}} I_{\text{eff}}}$$

where the subscripts denote the different layers. Since the barrel hangs vertically, there is no distributed gravity load, so $w_1 = w_2 = w_3 = w_{\text{eff}}$ for any transverse distributed load. This results in

$$E_{\text{eff}} I_{\text{eff}} = E_1 I_1 + E_2 I_2 + E_3 I_3$$

The resultant effective density calculated equals $35.7 \times 10^6 \text{ lb/in}^2$.

INTERIOR BALLISTIC MODELING

One of the most significant differences between the EM railgun and the conventional gun system is the means of providing the propulsive force. However, the RASCAL code allows for interior ballistic data to be input as velocity versus time and is thus transparent to the mode of propulsion.

Two separate interior ballistic curves were used in the analysis and are shown in Figure 4. The first curve, and the more severe case, shows a peak velocity of 1965 m/s at muzzle exit. This curve was provided by UTCEM from a simulation code developed in-house. It is important to realize this simulation does not accurately reflect the current status of the UTCEM gun system for large caliber projectiles. At the present time, rise times of about 100 microseconds are typical, with efforts ongoing to control the staging of generators to reduce the rise time to that shown in the simulation. Therefore, this curve represents an optimal interior ballistic loading from the EM railgun.

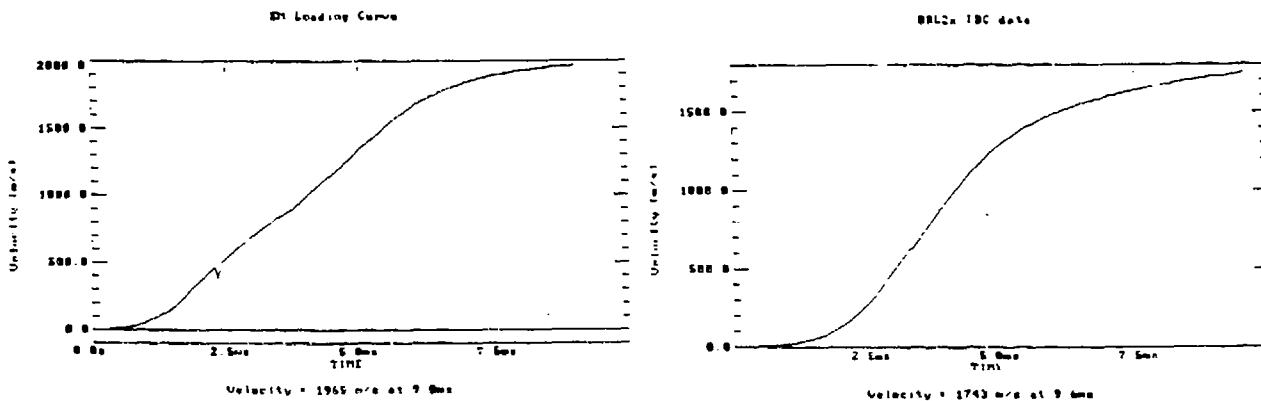


Figure 4. Interior Ballistic Curves used in RASCAL Analysis

The second load profile is for an M829 projectile fired from a double-travel cannon and does not include any charge optimization. This case achieves a maximum velocity of 1743 m/s at exit.

PROJECTILE GEOMETRY

RASCAL was written for specific application to projectiles operating in conventional tank cannons. Some of the assumptions required to apply the code to EM railgun cases have been detailed previously in the gun barrel modeling section. Similarly, a set of assumptions was required in modeling the EM projectile with RASCAL.

Two generic geometries are available within RASCAL for modeling projectiles. They are a double-ramp configuration as found in the M829 and the geometry of a Heat round. The EM projectile of interest is shown in Figure 5 and has the basic double-ramp configuration with two trailing armature contacts attached. Modeling these two trailing arms presents a difficulty since RASCAL's input is in the form of various tapers and a forward borerider as shown in Figure 6.



Figure 5. EM Projectile Configuration

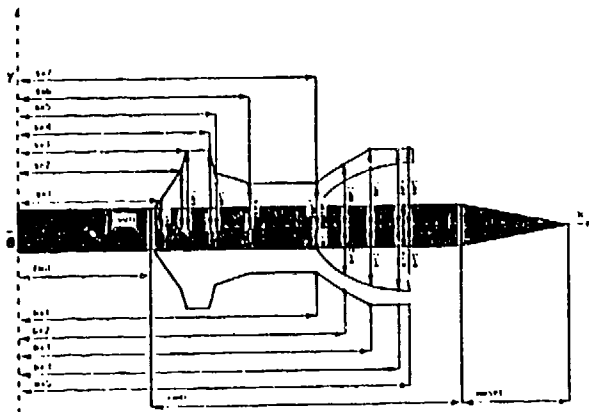


Figure 6. RASCAL Input Geometry for a Double-Ramp Sabot

The RASCAL model of the EM projectile is depicted in Figure 7. The swept-back portion of the chevron armature design is not included because of the limitations of the RASCAL geometry modeler. However, it was felt that the overhanging structure provides only minimal additional lateral stiffness, so that the model would yield a response fairly representative of the projectile.

Some preliminary calculations were also made to investigate the possibility of reversing the projectile direction to model one of the armature leaves by taking advantage of the forward borerider modeling capability (see Figure 8). However, from these calculations, this technique was determined to be unfeasible for this geometry because of the way RASCAL resolves the bore-riding structure into beam elements. Therefore, the representation shown in Figure 7 was chosen to best serve as the EM projectile model.

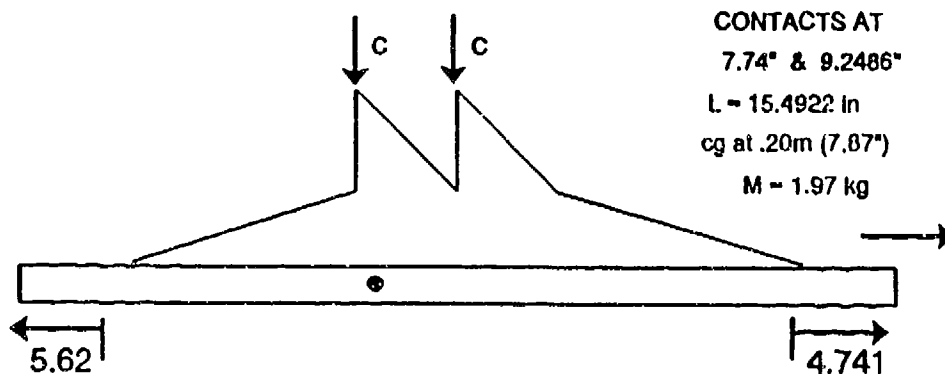


Figure 7. RASCAL Model of EM Projectile

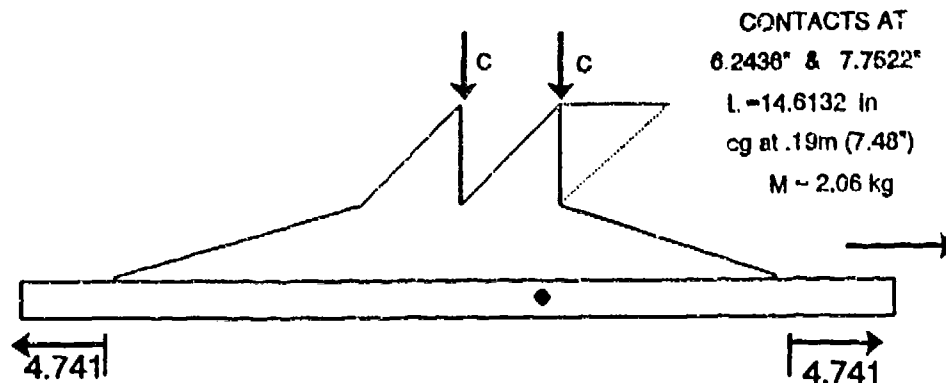


Figure 8. Alternate Model of the EM Projectile

The other projectile incorporated in the study was the M829, which is a standard ammunition for the 120-mm cannon. This was meant to serve as a baseline performer against which the EM design could be evaluated.

A key parameter in determining a projectile's in-bore performance is the stiffness associated with the projectile/bore interface. Attempts have been made to experimentally determine this contact stiffness value [7,8] with results ranging from approximately 1.0×10^5 to 1.0×10^6 lb/in in magnitude. Previous experience in matching the RASCAL output results with test firing data led to the use of 4.3×10^5 lb/in as a standard value [9]. For the purpose of this investigation, three different contact stiffness values were evaluated for each case studied to represent the lowest measured value (1.0×10^5 lb/in), the highest measured value (1.0×10^6), and a value used in previous evaluations with RASCAL (4.3×10^5 lb/in).

CASE STUDY MATRIX

The analysis involved the two projectile models with system parameters varied to look at 11 different scenarios as listed in Table 1. Each of the 11 cases were run with the three different stiffness values resulting in a total of 33 individual cases being investigated.

The study was set up so that Case 1 represented an estimate of the M829 projectile response from the double-travel gun having a conventional pressure profile loading. Case 2 was run to see how the more severe EM loading profile would affect the projectile. The third case isolated the effects attributable to the rail centerline, while Cases 4 and 5 provided data for the M829 in the EM gun system with rail and insulator centerlines, respectively. A final case, Number 11, was run during conditions similar to Case 1 except for use of the vertical centerline of the conventional double-travel gun instead of the horizontal centerline.

The other half of the investigation focused on the response of the EM projectile, with Case 6 serving as a baseline for the complete EM system. As with the M829 projectile cases, parameters were shuffled to see how singular changes affected in-bore

performance. Case 7 subjected the EM design to the conventional loading in the EM system. Case 8 examined the projectile's actions in an EM system having the double-travel gun's centerline. Case 9 analyzed the EM projectile in the conventional gun system, while Case 10 looked at projectile response in the EM system with the insulator centerline.

	Projectile	Loading	Centerline	Gun System	Barrel Geometry
Case 1	M829	Conventional	Double Travel 120mm	Double Travel Cannon	Double Travel Cannon
Case 2	M829	EM Profile	Double Travel 120mm	Double Travel Cannon	Double Travel Cannon
Case 3	M829	Conventional	UTCCEM Rails	Double Travel Cannon	Double Travel Cannon
Case 4	M829	EM Profile	UTCCEM Rails	UTCCEM	UTCCEM
Case 5	M829	EM Profile	UTCCEM Insulator	UTCCEM	UTCCEM
Case 6	EM	EM Profile	UTCCEM Rails	UTCCEM	UTCCEM
Case 7	EM	Conventional	UTCCEM Rails	UTCCEM	UTCCEM
Case 8	EM	EM Profile	Double Travel 120mm	UTCCEM	UTCCEM
Case 9	EM	Conventional	Double Travel 120mm	Double Travel Cannon	Double Travel Cannon
Case 10	EM	EM Profile	UTCCEM Insulator	UTCCEM	UTCCEM
Case 11	M829	Conventional	Double Travel 120mm (vertical)	Double Travel Cannon	Double Travel Cannon

Table 1. Listing of Parameters for Each Case Investigated

RESULTS

The output from RASCAL includes a wealth of information to determine both projectile and gun response. The focus of this effort was on the in-bore response of the round so the information extracted and examined from the RASCAL output included the transverse velocity at the projectile center of gravity and the projectile's angular velocity over the length of in-bore travel.

The transverse acceleration of each projectile's center of gravity was determined by taking a derivative of the RASCAL calculated velocity with a subsequent conversion made into g's. These values are tabulated in Table 2 for the 11 cases examined for all three contact stiffness values. Figure 9 is a graphical display of the same information. While the EM projectile cases generally exhibit higher transverse accelerations, they are the same order of magnitude as the M829 cases. The disturbing fact of these results is the dramatic rise in lateral acceleration for both projectiles traveling through the EM gun with the insulator centerline (Cases 5 and 10). The M829 cases exhibit increasing accelerations as the contact stiffness is increased. This is to be expected since the projectile's center of gravity is beneath the rear contact so that any increasing force transmitted through the stiffer contact acts directly on the center of gravity. Conversely, the EM projectile has its center of gravity between the two contact points. The data reveal the medium stiffness value ($4.3\text{e}05$ lb/in) results in more aggravated transverse accelerations than the stiffest contact ($1.0\text{e}06$ lb/in). This may be because one of the rod's natural bending frequencies is excited when the medium stiffness is used.

Maximum Transverse Acceleration, g's							
k, lb/in	1.0e05	4.3e05	1.0e06	k, lb/in	1.0e05	4.3e05	1.0e06
Case 1	534	649	1492	Case 6	1882	3152	2142
Case 2	552	857	1615	Case 7	1722	3215	1941
Case 3	247	845	2406	Case 8	1442	1563	2139
Case 4	296	1249	2585	Case 9	1185	1517	1122
Case 5	884	1868	8498	Case 10	2227	5973	4321
Case 11	211	591	673				

Table 2. Maximum Transverse Accelerations

It is also interesting to notice the trends in the magnitude of the transverse acceleration values. In proceeding from left to right on Figure 9, Cases 1 through 5 show increasing peak lateral accelerations. This corresponds to the M829 being subjected to more "EM-like conditions" with each subsequent case. That is, Case 1 employs a conventional gun system, Cases 2 and 3 have some aspects of the EM system integrated, and Cases 4 and 5 have the M829 in a full EM environment. Case 11 reinforces this notion that the conventional system produces a more benign response.

Similarly, Cases 6 through 9 show that as the EM projectile is introduced to more elements of the conventional gun system (again, moving left to right), it alleviates the severity of the transverse acceleration. Case 10 serves as a stark contrast to its predecessor, Case 9, pointing out the differences between the conventional system and the EM system with the insulator centerline.

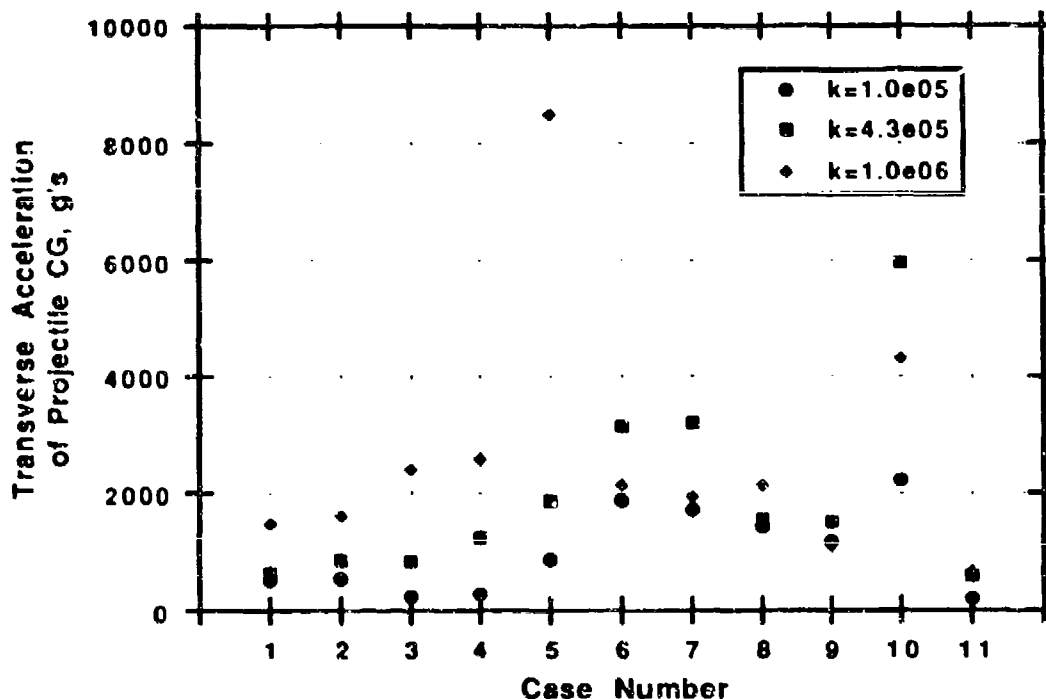


Figure 9. Comparison of Transverse Accelerations

The other output examined from the RASCAL analysis was the data for the angular rate of the projectile. These data are a measure of the instantaneous velocity of the projectile model slope, based on the displacement of the contact points. This provides a feel for the magnitude of a projectile's yawing motion while in bore. Plots of the angular velocity versus time are presented in Figures 10 through 42 for the 11 case studies with the various contact stiffness values.

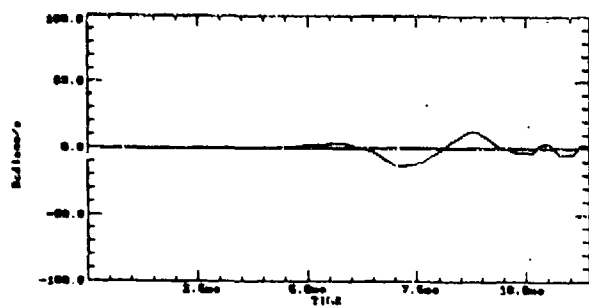


Figure 10. Angular Velocity of Case 1
h=1.0e05 lb/in

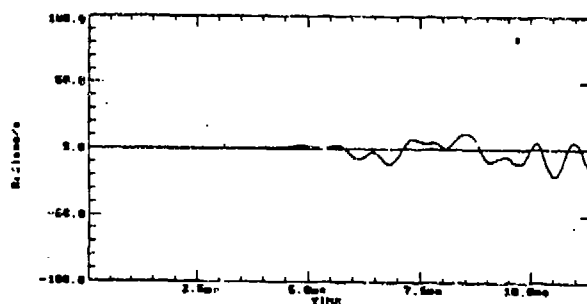


Figure 11. Angular Velocity of Case 1
h=4.0e05 lb/in

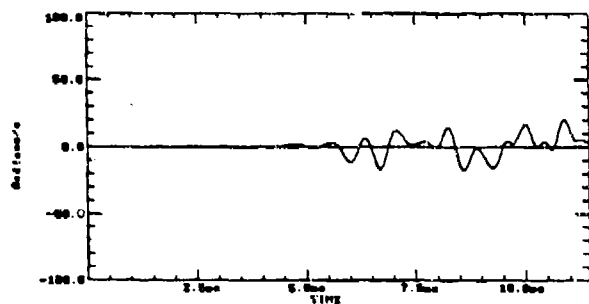


Figure 12. Angular Velocity of Case 1
h=1.0e06 lb/in

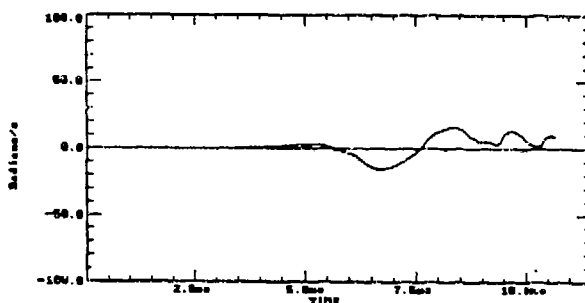


Figure 13. Angular Velocity of Case 2
h=1.0e05 lb/in

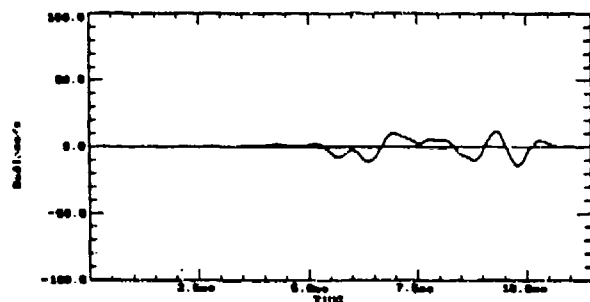


Figure 14. Angular Velocity of Case 2
h=4.0e05 lb/in

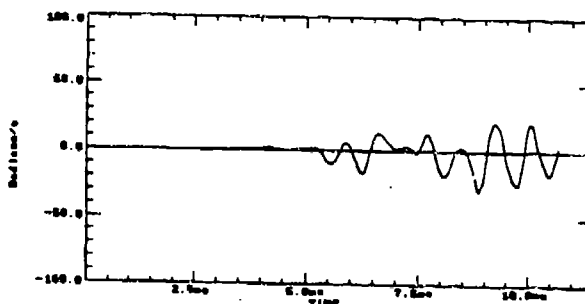


Figure 15. Angular Velocity of Case 2
h=1.0e06 lb/in

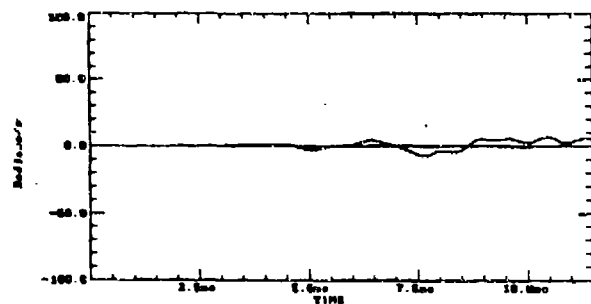


Figure 16. Angular Velocity of Case 3
h=1.0e05 lb/in

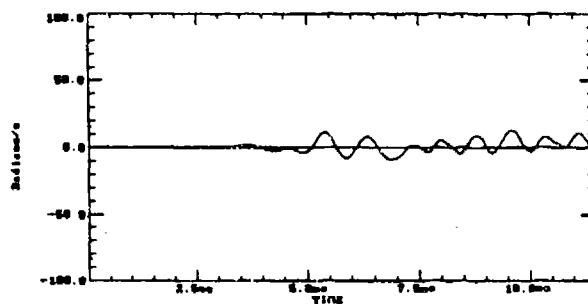


Figure 17. Angular Velocity of Case 3
h=4.0e05 lb/in

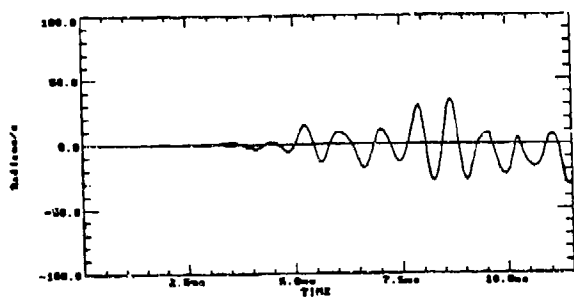


Figure 18. Angular Velocity of Case 2
h=1.0e06 lb/in

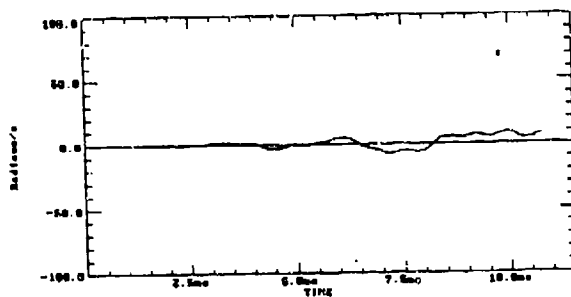


Figure 19. Angular Velocity of Case 4
h=1.0e06 lb/in

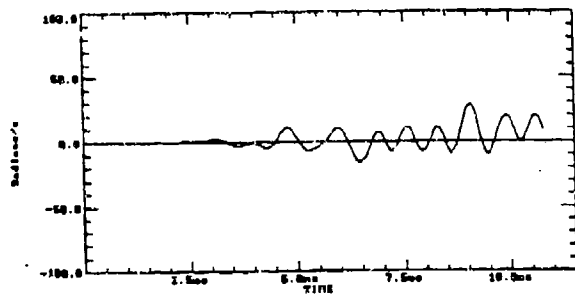


Figure 20. Angular Velocity of Case 4
h=4.3e05 lb/in

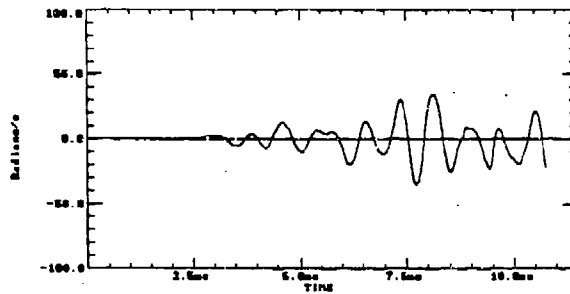


Figure 21. Angular Velocity of Case 4
h=1.0e06 lb/in

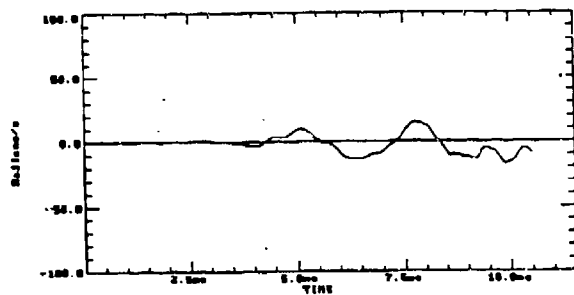


Figure 22. Angular Velocity of Case 5
h=1.0e06 lb/in

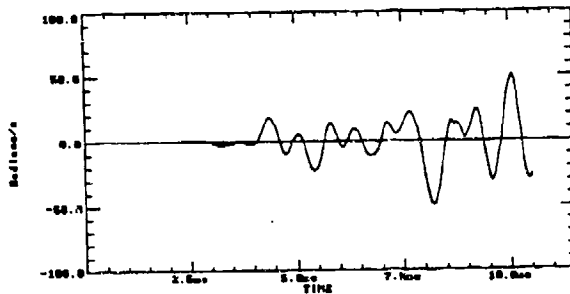


Figure 23. Angular Velocity of Case 5
h=4.3e05 lb/in

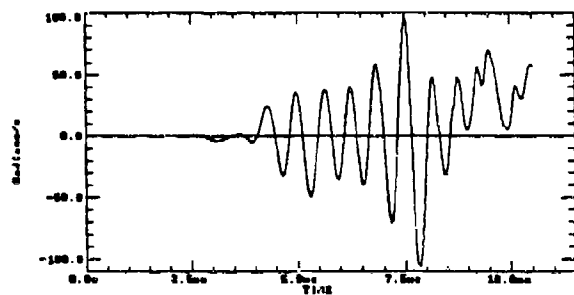


Figure 24. Angular Velocity of Case 5
h=1.0e06 lb/in

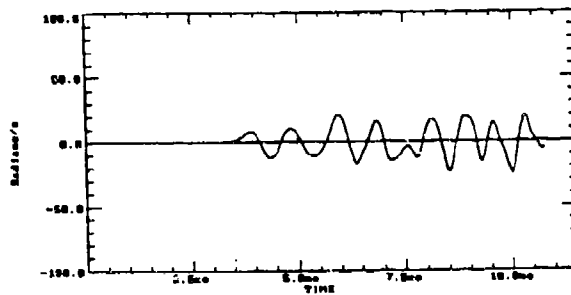


Figure 25. Angular Velocity of Case 6
h=1.0e06 lb/in

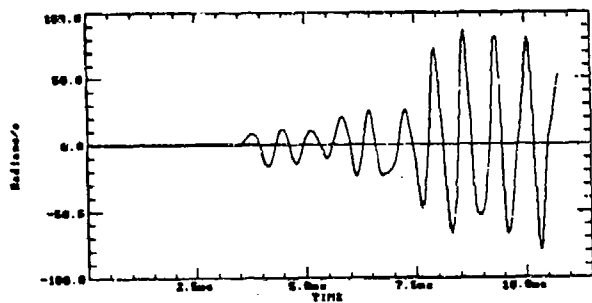


Figure 25. Angular Velocity of Case 6
h=4.3e05 lb/in

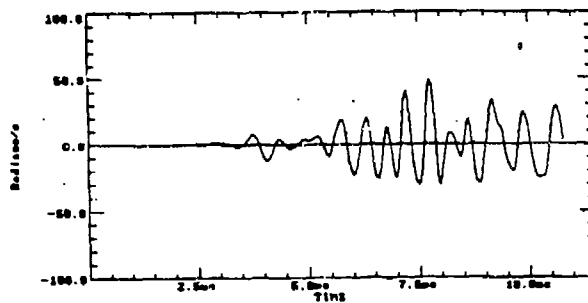


Figure 27. Angular Velocity of Case 6
h=1.0e06 lb/in

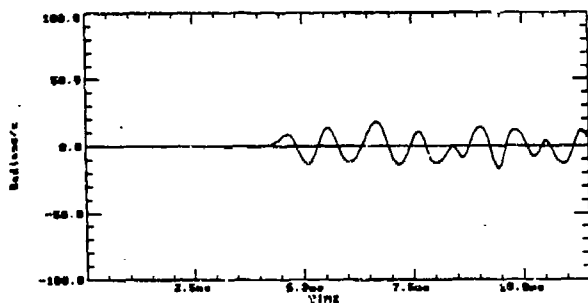


Figure 29. Angular Velocity of Case 7
h=1.0e05 lb/in

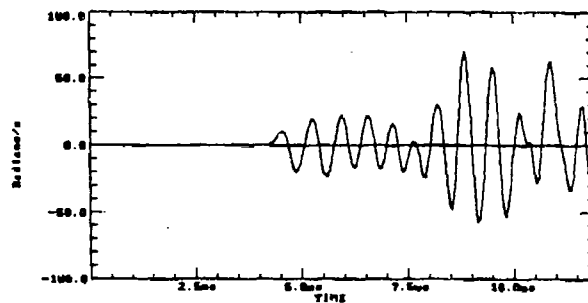


Figure 29. Angular Velocity of Case 7
h=4.3e05 lb/in

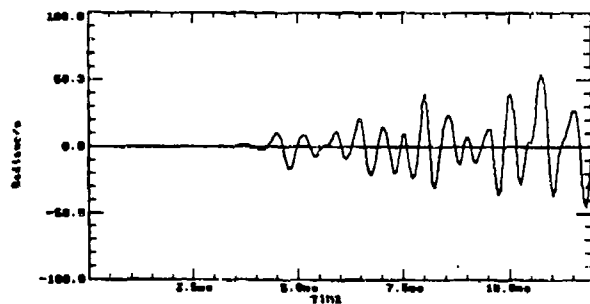


Figure 30. Angular Velocity of Case 7
h=1.0e05 lb/in

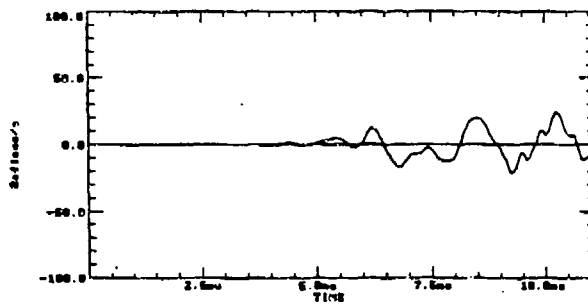


Figure 31. Angular Velocity of Case 8
h=1.0e05 lb/in

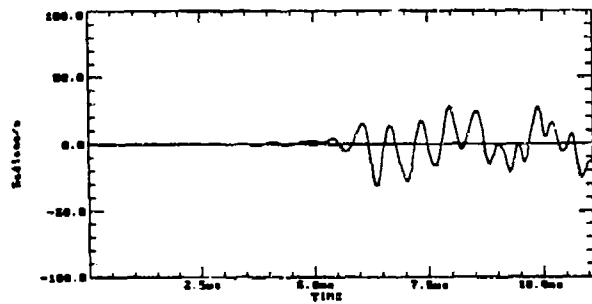


Figure 32. Angular Velocity of Case 8
h=4.3e05 lb/in

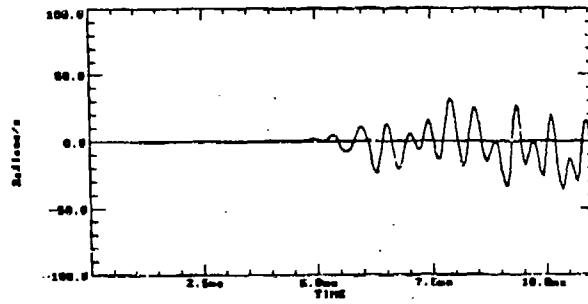


Figure 33. Angular Velocity of Case 8
h=1.0e05 lb/in

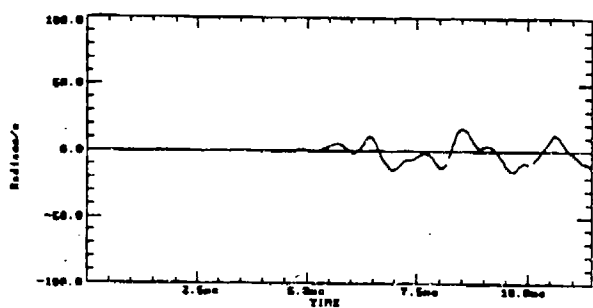


Figure 34. Angular Velocity of Case 9
 $h=1.0e05$ lb/in

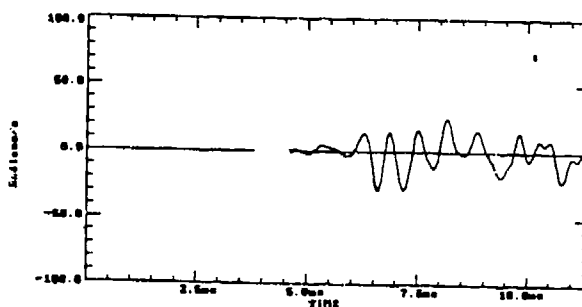


Figure 35. Angular Velocity of Case 9
 $h=4.3e05$ lb/in

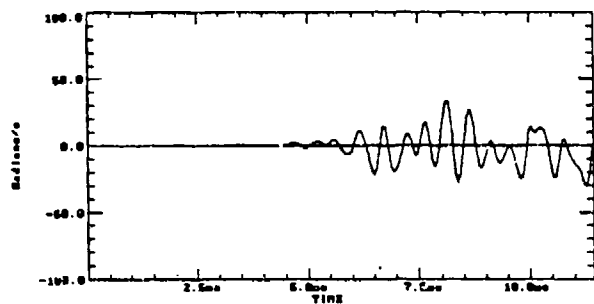


Figure 36. Angular Velocity of Case 9
 $h=1.0e06$ lb/in

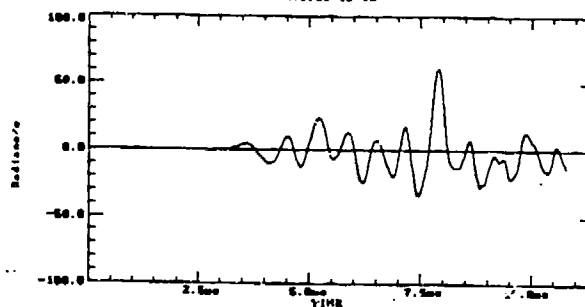


Figure 37. Angular Velocity of Case 10
 $h=1.0e05$ lb/in

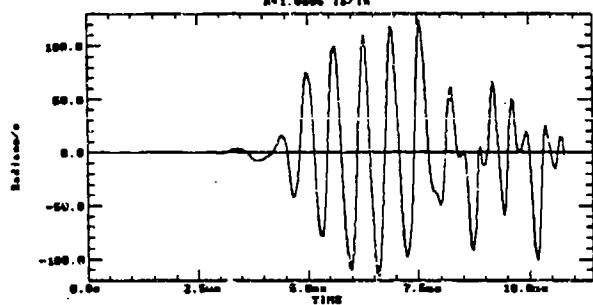


Figure 38. Angular Velocity of Case 10
 $h=4.3e05$ lb/in

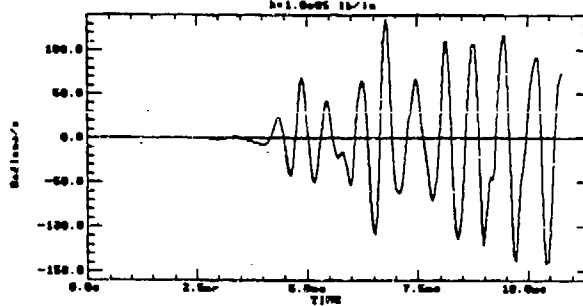


Figure 39. Angular Velocity of Case 10
 $h=1.0e06$ lb/in

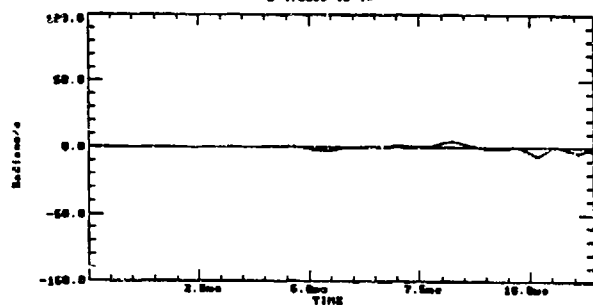


Figure 40. Angular Velocity of Case 11
 $h=1.0e05$ lb/in

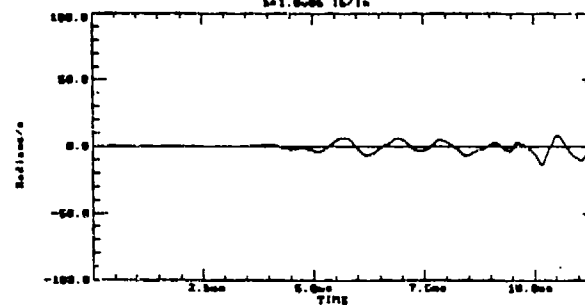


Figure 41. Angular Velocity of Case 11
 $h=4.3e05$ lb/in

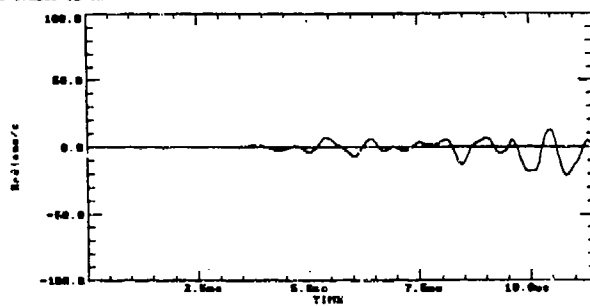


Figure 42. Angular Velocity of Case 11
 $h=1.0e06$ lb/in

From the plots, it is seen that the M829 with the soft contacts ($k=1.0e05$ lb/in) yields a rather benign response for all cases (Cases 1 through 5, and 11). By comparing Cases 1 and 3 with Cases 2 and 4, respectively, one finds the projectile motion is mostly unaffected by a change in load profile. Substitution of the rail centerline profile for the conventional double-travel (Case 1 vs. Case 3 and Case 2 vs. Case 4) reveals a slight exacerbation of the in-bore motion. In general, the yawing motion worsens with an increase in contact stiffness. The case of the M829 through the EM insulator centerline, Case 5, is clearly the poorest performer from any of the analysis runs with this projectile.

The EM projectile cases exhibit trends comparable to those with the M829. Namely, the insulator centerline subjects the round to the most severe angular velocity, while the EM rail profile shows only slightly worse results than the conventional gun case does. Also, it is noted how a change in interior ballistic loading results in little difference between the EM and conventional cases. These EM projectile cases have an increasingly higher angular velocity when going from the soft to medium contacts, but the magnitude of the angular rate levels off and does not increase for the stiffest contacts. This is another indication that the medium contact stiffness excites a natural bending frequency of the rod.

In comparing the EM projectile to the M829, it is seen that the EM round has consistently higher angular rates for the soft contact cases. Also, given the conventional gun centerline, both projectiles show angular velocities of equivalent magnitude. Thus, nothing appears to be inherent in the different projectile designs that aggravates the in-bore yaw.

CONCLUSIONS

From this analysis, it is clear the EM gun system presents a more severe environment than does a conventional powder gun. The results point to the difference in centerlines as a primary cause. Changes in interior ballistic input are shown to have little effect on the transverse acceleration and angular velocity over the length of in-bore travel. However, further studies are required to ascertain if this holds true for velocities well above those of today's ordnance (2.5 km/s and up, for instance).

The differences between the M829 and EM projectile geometries do not greatly influence the in-bore yawing motion. In general, the EM projectile is consistently subjected to larger transverse accelerations, but the delta is minimal. Also, the apparent tendency to excite natural frequencies of the subprojectile for the medium spring stiffness case is certainly something that the EM projectile designer must concern himself with and try to avoid.

The choice of the gun barrel centerline profile acts as the principal driver in determining the projectile response for this

study. While the rail profile results in yawing motion only slightly worse than the powder gun, the insulator profile clearly brings about the worst response, with both the transverse accelerations and angular velocities being substantially higher.

The one-dimensionality of the RASCAL analysis fails to account for any coupling effects that result from traversing the rail and insulator centerlines simultaneously. Since it has been shown that the rail centerline imparts more motion to the projectile than a conventional gun does, and the insulator centerline produces even greater motion, it is feared that a more advanced code capable of modeling the full internal bore geometry will show even more deleterious results.

Finally, the results of this analysis point out a weakness of the current EM gun systems. an inability to maintain a relatively benign centerline through which the projectile traverses. At present, EM railguns have centerlines that fluctuate from shot to shot. Until a consistent, less severe centerline profile can be maintained, EM projectiles will have difficulty matching the in-bore, and subsequently, the flight and terminal performance of rounds fired from conventional guns.

REFERENCES

1. T.F. Erline, M.D. Kregel, and M. Pantano, "Gun and Projectile Flexural Dynamics Modeled by the Little RASCAL - a User's Manual", BRL-TR-3122, U.S. Army Ballistic Research Laboratory, Aberdeen Proving Ground, MD, July 1990.
2. T.F. Erline, M.D. Kregel, "Flexible Projectile Modeling Using the Little RASCAL Gun Dynamics Program", Proceedings of the Sixth U.S. Army Symposium on Gun Dynamics, Tamiment, PA, May 1990.
3. D.A. Hopkins, "Modeling Gun Dynamics with Three-Dimensional Beam Elements", Proceedings of the Sixth U.S. Army Symposium on Gun Dynamics, Tamiment, PA, May 1990.
4. N.D. Manners, "A Theoretical Study into the Effect of Sabot Stiffness on Projectile In-Bore Motion and Launch Accuracy", Proceedings of the Sixth U.S. Army Symposium on Gun Dynamics, Tamiment, PA, May 1990.
5. M.A. Polcyn, P.A. Cox, "The Adaptation of NASTRAN for Three-Dimensional Gun Dynamics Problems", Proceedings of the Sixth U.S. Army Symposium on Gun Dynamics, Tamiment, PA, May 1990.
6. D.A. Rabern, K.A. Bannister, "Finite Element Models to Predict the Structural Response of 120-mm Sabot/Rods During Launch", Proceedings of the Sixth U.S. Army Symposium on Gun Dynamics, Tamiment, PA, May 1990.

BURTON

7. D.H. Lyon, "Radial Stiffness Measurements of 120-mm Projectiles", U.S. Army Research Laboratory, Aberdeen Proving Ground, MD, to be published.
8. C.D. McCall, D.L. Henry, "Flexural Characteristics of the M829 Projectile Family", U.S. Army Research Laboratory, Aberdeen Proving Ground, MD, to be published.
9. T.F. Erline, "Projectile Spring Constants Significance to Modeling with the Little RASCAL Gun Dynamics Program", BRL-TR-3224, U.S. Army Ballistic Research Laboratory, Aberdeen Proving Ground, MD, April 1991.